RSC Advances

This article can be cited before page numbers have been issued, to do this please use: V. S. Koneni, L. R. Singh, D. Choudhary, A. Arun, S. Gupta, S. Adhikary, G. R. Palnati, R. Konwar and R. trivedi, *RSC Adv.*, 2016, DOI: 10.1039/C6RA15674F.

ROYAL SOCIETY OF CHEMISTRY

www.rsc.org/advances

Dynamic Article Links ►
View Article Online
DOI: 10.1039/C6RA15674F

Cite this: DOI: 10.1039/c0xx00000x

www.rsc.org/xxxxxx

ARTICLE TYPE

Design, synthesis and *in-vitro* evaluation of coumarin-imidazo[1,2-*a*]pyridine derivatives against cancer induced osteoporosis

Koneni V. Sashidhara,*[a] L. Ravithej Singh,[a] Dharmendra Choudhary,[b] Ashutosh Arun,[b] Sampa Gupta,[a] Sulekha Adhikary,[b] Gopala Reddy Palnati,[a] Rituraj Konwar[b] and Ritu Trivedi[b]

Received (in XXX, XXX) Xth XXXXXXXXX 20XX, Accepted Xth XXXXXXXXX 20XX
DOI: 10.1039/b000000x

A series of biologically important 6-(imidazo[1,2-*a*]pyridin-2-yl)-2*H*-chromen-2-one derivatives were synthesized by employing the silver (I) catalysed Groebke-Blackburn-Bienayme multicomponent reaction. Synthesized compounds were tested against primary calvarial osteoblast differentiation assay and alizarin red-S staining assay for their possible osteoprotective properties. Further, the effect of active compounds **6h**, **6l**, and **6o** on the expression of osteogenic genes *BMP2*, *RUNX2*, *COL1*, and *OCN* were measured by qPCR. Out of three promising compounds, **6l** and **6o** significantly induced apoptosis in MDA-MB-231 cancer cells *via* mitochondrial depolarisation without affecting normal cells. In an *in-vitro* co-culture model of bone metastasis, we investigated the ability of coumarin-imidazo[1,2-*a*]pyridine hybrids to reverse the negative impact of MDA-MB-231 cancer cells on osteoblast differentiation. The results illustrate the potential of designed hybrids to re-establish the bone homeostasis. These findings demonstrate the significance of newly synthesized hybrids as lead molecules, possessing both antiosteoporotic and anticancer properties that can be developed into new therapeutic agents to alleviate osteoporosis and bone metastasis.

1. Introduction

Bone is a dynamic organ that is actively engaged in resorption and rebuilding process throughout the individual's life. Osteoclast and osteoblast play a central role in maintaining skeletal integrity by a well-organised resorption and deposition processes, called bone remodeling.[1] The impair function of this homeostatic regulation process leads to loss of bone mass and weakening of bone micro architecture resulting in a skeletal disorder called osteoporosis.[2] Osteoporotic bone loss also occurs by inflammation, adipokines, and cancer metastasis and these are widely recognized as a major threat to public health.[3] The tendency of cancerous cells to disengage from primary tumor and invade the other organs in the body, through the circulatory system, to develop as secondary cancer is called metastasis.[4] Notably, many different types of cancer cells lead to bone loss and fracture by metastasizing to bone. In 70% of breast cancer patients, bone metastasis is observed which in turn lead to bone deterioration with severe pathological skeletal fractures and unrelenting pain.[5] In the course of osteoporosis, up-regulation of osteoporotic process in bone microenvironment results in the secretion of systemic factors like parathyroid hormone and local factors such as TNF-α, TGF-β and interleukins in excessive quantities that subsequently increase the osteoclast production and activity.[6] These processes make the skeleton fragile and favor the progression of metastatic cancer in bone. As revealed in "seed and soil hypothesis," the growth factors produced by disseminated tumor cells triggers the osteoclast activity that sequentially releases bone-derived growth factors to promote the growth of metastasized tumors.[7] This bidirectional interaction of resorption site and colonised tumor cells turns bone microenvironment congenial for the progression of skeletal damage.

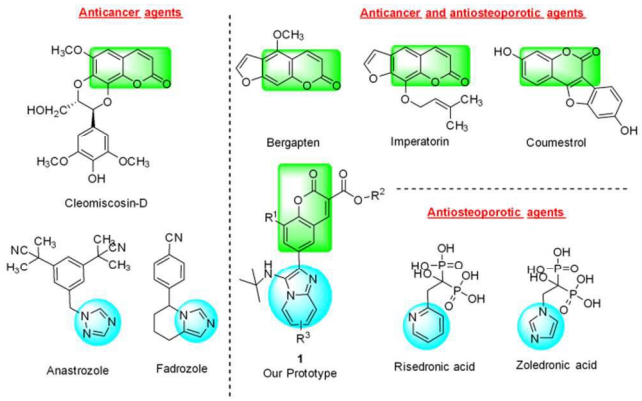

Fig. 1 Chemical structures of representative coumarin and nitrogen heterocyclic compounds with potent anti-cancer and anti-osteoporotic activities and general structure of our designed prototype.

Bisphosphonate therapy is first-line medication recommended by the World Health Organization for treating osteoporosis, however it is associated with adverse side-effects.[8] Calcitonin is approved FDA drug for postmenopausal women, which is associated with complications such as blurred vision, muscle cramps, nausea, and

View Article Online
DOI: 10.1039/C6RA15674F

seizures. The recombinant parathyroid hormone, teriparatide,[9] is an anabolic agent for the treatment of high risk of fracture associated with osteoporosis, for both men and women, to increases the bone mass. However, it cannot be administered to the patients with bone metastasis and osteosarcoma as it cause cancer relapse. Calcitriol, sodium fluoride, strontium ranelate, tibolone, other bisphosphonates (etidronate, pamidronate, tiludronate) and combination therapies[10] are at different phases of clinical trials and yet to be approved by FDA. Therefore, it is desirable to have new agents that can tackle osteoporosis as well as metastasise-induced bone loss.

Coumarins belong to benzo-*α*-pyrone class of compounds and have been found to exhibit a variety of pharmacological activities. The natural product cleomiscosin A,[11] is found to exhibit *in vivo* anticancer activity. While other naturally occurring coumarin derivatives like coumestrol,[12] imperatorin, and bergapten[13,14] are known to possess both antiosteoporotic and anticancer activity. On the other hand, nitrogen containing heterocyclics like fadrozole and anastrozole are known anticancer drugs that are in current use.[15] Also, a large body of evidence support the use of these aromatase inhibitors as adjuvant therapeutics for breast cancer in postmenopausal women,[16] whereas nitrogen containing bisphosphonates, such as risedronic acid and zoledronic acid are used to treat metastatic bone cancer in a combination therapy for both pre and postmenopausal women.[17] (Fig. 1)

Taken as a whole, monotherapy is not successful in treating bone loss and metastasis simultaneously, while combination therapy has practical limitations of drug-drug interactions, dosing, bioavailability and unpredictable pharmacokinetic actions.[18] Pharmacophore hybridization is a new paradigm in medicinal chemistry for designing of novel molecular frameworks.[19] Among the existing methodologies for combining coumarin-imidazole scaffold, Manver *et. al*. demonstrated the synthesis of coumarin-imidazole hybrids by utilizing the Groebke-Blackburn-Bienayme multicomponent reaction and predicted their NS5B inhibitor potential by means of molecular docking studies.[20] On the other hand, Karamthulla *et al* reported an elegant synthesis of disubstituted imidazo[1,2-a]pyridine derivatives by employing arylglyoxals, cyclic 1,3-dicarbonyls and 2-aminopyridines under microwave irradiation.[21] In our earlier lab work, we reported the synthesis and osteoporotic potential of coumarin−pyridine hybrids against postmenopausal osteoporosis.[22] On the basis of these previous findings, in the present study we designed and synthesized coumarin-imidazo[1,2-*a*]pyridine hybrids (**1**, Fig. 1) and evaluated their potential against cancer induced osteoporosis.

2. Chemistry

The synthesis of coumarin-imidazo[1,2-*a*]pyridine hybrid molecules were achieved by synthetic route shown in Scheme 1. In the first step, *o*-alkyl substituted phenols were subjected to the Duff formylation with hexamethylenetetramine (HMTA) in trifluoroacetic acid as a solvent followed by acid hydrolysis with 10% aq H_2SO_4 furnishing 4-hydroxy-5-alkylisophthalaldehyde (**3a-d**).[23] These *iso*phthalaldehyde intermediates were then subjected to piperidine catalysed Knoevenagel condensation with ethyl/methyl acetoacetates to yield corresponding coumarin esters (**4a-g**).[22]

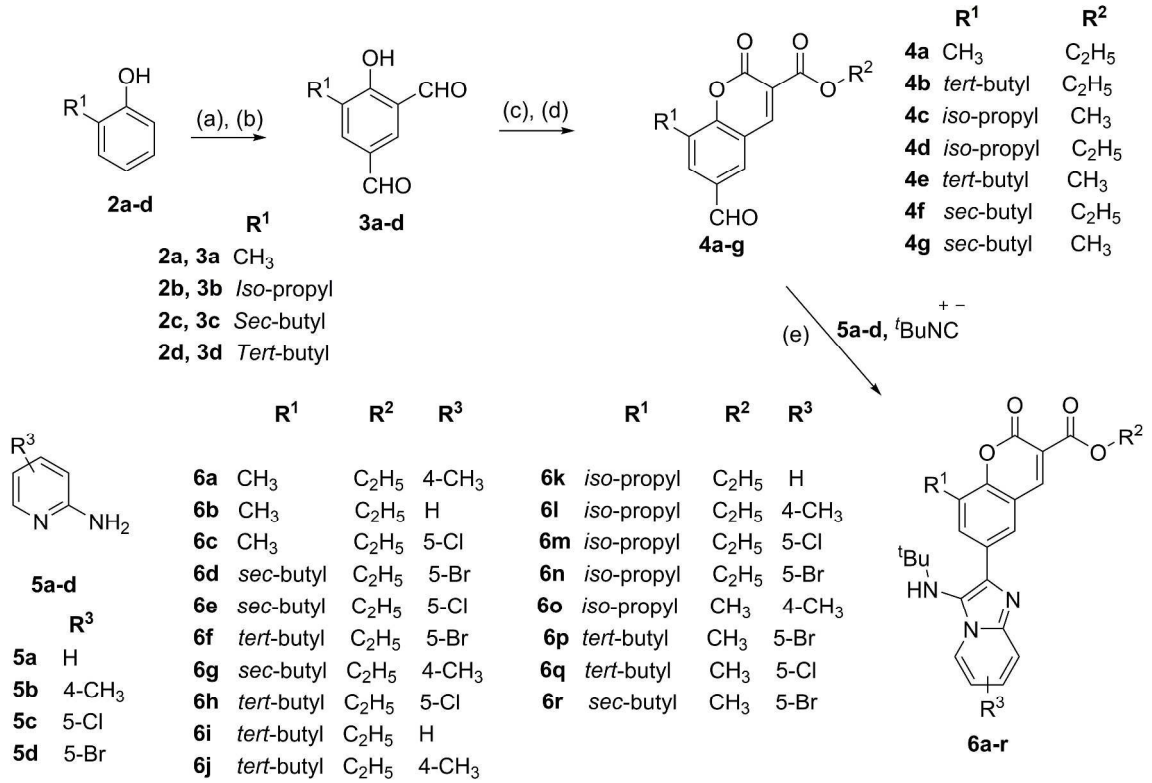

Scheme 1 Reagent and conditions: (a) HMTA, TFA, 120 °C, 4 h; (b) aq H_2SO_4, 100 °C, 2 h; (c) diethyl/methyl malonate, EtOH, piperidine, reflux, 30 min; (d) Glacial acetic acid, rt.; (e) Ag(OTf), ethanol, reflux, 6 h.

View Article Online
DOI: 10.1039/C6RA15674F

Table 1 Optimisation of reaction conditions[a]

Entry	Catalyst (equiv)	Time (hrs)	Yields[b]
1	$BiCl_3$ (20 mol%)	6	26
2	$FeCl_3$ (20 mol%)	6	18
3	$CoCl_2$ (20 mol%)	6	22
4	$ZrCl_4$ (20 mol%)	6	65
5	$SnCl_4$ (20 mol%)	6	42
6	AgOTf (20 mol%)	6	86
7	AgOTf (10 mol%)	6	68
8	AgOTf (10 mol%)	4	62
9	AgOTf (10 mol%)[c]	6	45
10	AgOTf (10 mol%)[d]	10	18
11	AgCl (20 mol%)	6	36
12	No Catalyst	12	-

[a] **Reaction conditions**: 2-Amino-4-picoline (**5b**), ethyl-6-formyl-8-methyl-2-*oxo*-2*H*-chromene-3-carboxylate (**4a**) and *tert*-butyl isocyanide in ethanol. [b] isolated yields, [c] 50 °C temperature, [d] room temperature.

Finally, the Groebke-Blackburn-Bienayme multicomponent reaction was employed for the synthesis of target compounds. However, the reported procedures[24] by using ethyl 6-formyl-8-methyl-2-*oxo*-2*H*- chromene-3-carboxylate (**4a**), 2-Amino-4-picoline (**5b**) and *tert*-butyl isocyanide as reactants for model example resulted in low yields. Therefore, we set out to optimise new synthetic protocol for the synthesis of designed coumarin-imidazo[1,2-*a*]pyridine conjugates in good yields. Initially we investigated the role of different metal catalysts including $BiCl_3$, $FeCl_3$, $CoCl_2$, $SnCl_4$, $ZrCl_4$ and Ag(OTf) to carry out the reaction in ethanol as a solvent. Among the screened catalysts, silver (I) triflate was found to be effective at 80 °C reaction temperature.

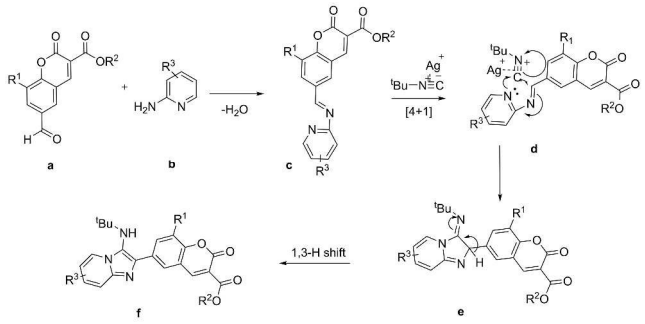

Scheme 2 Plausible reaction mechanism of imidazo[1,2-*a*]pyridine synthesis.

A brief screening of solvents showed ethanol as suitable solvent and further increase in reaction temperature neither reduced reaction time nor improved yield (Table 1). The substituted 2-aminopyridine with, both, electron-donating as well as electron-withdrawing groups underwent the cyclization smoothly under the optimised reaction conditions. The catalytic role of Ag(I) is shown in the plausible mechanism outlined in scheme. 2.[25] Initially, aldehyde (**a**) and 2-aminopyridine (**b**) react spontaneously in the reaction medium to give corresponding imine (**c**,). Subsequently, Ag(I) activates the *tert*-butyl isocyanide and promotes it to attack on imine which further undergo series of electronic transformations (**d** and **e**) eventually resulting in imidazo[1,2-*a*]pyridine (**f**) as a final product. The structures of all synthesized compounds were confirmed by mass spectrometry, IR, ^1H and ^{13}C NMR spectroscopy.

3. Results and Discussion

3.1. Coumarin-imidazo[1,2-*a*]pyridine hybrids stimulate the ALP activity and mineralization in primary osteoblast cells

All the synthesized compounds (**6a-6r**) were initially tested for their bone alkaline phosphatase (ALP) activity in osteoblast cells at a different concentration ranging from (10 pM to 1 μM). ALP is bound to osteoblast cell surfaces *via* a phosphor-inositol linkage and plays an important role in bone formation and is used as an indicator of bone formation in the screening of new osteogenic compounds. Among these, compounds **6h**, **6l**, and **6o** were found to stimulate the ALP activity in comparison to untreated cells as control. Compound **6h** at 1 μM ($P < 0.01$) and 10 nM ($P < 0.01$, compound **6l** at 1 μM ($P < 0.01$) and 10 nM ($P < 0.05$), and compound **6o** at 1 μM ($P < 0.05$) and 10 nM ($P < 0.01$), concentration significantly improved ALP activity (Fig. 2A).

Therefore, active compounds **6h** (1 μM and 10 nM), **6l** (1 μM and 10 nM), and **6o** (1 μM and 10 nM) were further studied for their effect on mineralization ability of osteoblast cells. Mineralization ability of compound is essential for the determination of osteogenic differentiation that mimics *in-vivo* bone hardness and strength. In mineralization process bone forming cells produce crystals of calcium phosphate, and these crystals lay down in bone matrix. Compound **6h** at 1 μM ($P < 0.01$) and 10 nM ($P < 0.001$), compound **6l** at 1 μM ($P < 0.05$) and 10 nM ($P < 0.05$), and compound **6o** at 1 μM ($P < 0.01$) and 10 nM ($P < 0.01$), concentration significantly enhanced mineralization as compared to untreated control (Fig. 2B). Furthermore, the active compounds **6h**, **6l**, and **6o** did not show any toxicity as compared to the control group at all treated concentrations (doses ranging from 1 μM to 10 nM) and were found to be safe, when evaluated by MTT assay in mice calvarial osteoblast cells (See supporting information. Fig. 1).

3.2. Effect of compounds on osteogenic gene expression

After mineralizing activity of compounds, further osteogenic potential of the compound at the transcriptional level was assessed by quantitative PCR of osteogenic genes *RUNX2*, *BMP2*, *COL1* and *OCN*. RUNX2 (Runt-related transcription factor 2) is a first transcription factor that is expressed in cells committed towards osteoblast lineages. Mesenchymal stem cells population of bone marrow stromal cells are the precursor cells for osteoblast, so up-regulation of RUNX2 indicates an upsurge in differentiation towards osteoblastic lineage. Bone morphogenetic proteins (BMPs) play a key role in the development and homeostasis of bone by inducing mesenchymal stem cells to differentiate into bone-forming cells. Among all bone morphogenetic proteins, BMP2 is an important factor in regulating bone remodelling and fracture healing. We also studied the effect of collagen type I (COL1) - the major constituent of bone matrix and bone gamma-carboxyglutamate

View Article Online
DOI: 10.1039/C6RA15674F

protein (OCN), the most abundant protein in osteoblasts cells that regulate bone homeostasis and help in binding to calcium and hydroxyapatite to bone. After analysing the real-time PCR data of calvarial osteoblast cells, we found that *BMP2*, *RUNX2*, *COL1*, and *OCN* mRNA expression were increased in the presence of compound **6h**, **6l**, and **6o**.

Compound **6h** at 1 μM increased BMP2 ($P < 0.001$), RUNX2 ($P < 0.001$), COL1 ($P < 0.001$) and OCN ($P < 0.001$) activity and at 10 nM concentration improved BMP2 ($P < 0.01$) and OCN ($P < 0.05$) as compared to untreated control after 48 h of treatment. Compound **6l** at 1 μM increased BMP2 ($P < 0.05$), RUNX2 ($P < 0.05$), COL1 ($P < 0.01$) and OCN ($P < 0.05$) activity and at 10 nM concentration improved BMP2 ($P < 0.05$) only. Compound **6o** at 1 μM increased BMP2 ($P < 0.05$), RUNX2 ($P < 0.001$), COL1 ($P < 0.01$) and OCN ($P < 0.05$) activity and at 10 nM concentration improved BMP2 ($P < 0.05$) and COL1 ($P < 0.01$) only (Fig. 3).

After identifying the osteogenic activity of compound **6h**, **6l** and **6o,** we proceeded to test the active compounds for anticancer activity in different cancer cell lines in order to explore their potency against cancer induced osteoporosis.

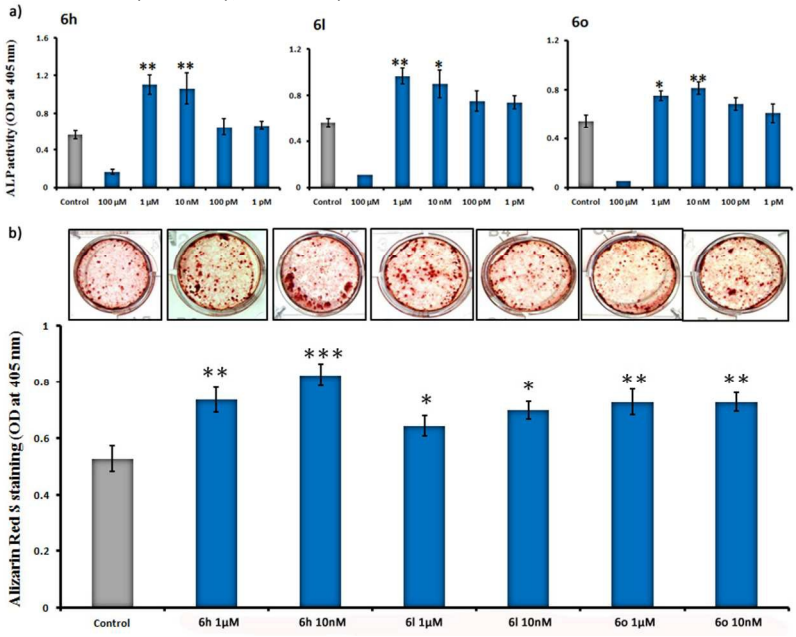

Fig. 2 a) alkaline phosphatase (ALP) activity in mice calvarial osteoblast cells of compounds **6h**, **6l** and **6o** after 48 hr of treatment. **b)** Effect of compound **6h**, **6l** and **6o** in mineralized nodule formation in mice calvarial osteoblast cells as observed by Alizarin Red-S staining.

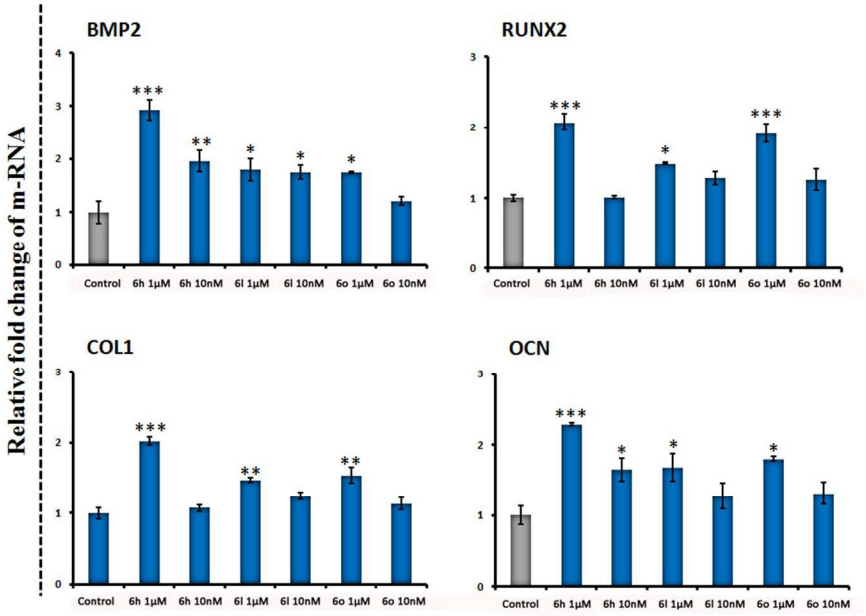

Fig. 3 Compounds **6h**, **6l** and **6o** on the expression of osteogenic genes (*BMP2*, *RUNX2*, *COL1* and *OCN*) in calvarial osteoblasts after 48 hr of treatment and as compared to control (non-treated cells) by qPCR.

View Article Online
DOI: 10.1039/C6RA15674F

3.3. Cancer cell inhibition assay

Compounds **6h**, **6l**, and **6o** were evaluated for cancer cell inhibition using MTT assay against breast cancer (MCF-7, MDA-MB-231) and cervical cancer (Ishikawa) cell line. Among the three test compounds, **6h** was inactive up to 50µM concentration and **6o** was most active against MDA-MB-231 cancer cells, with IC_{50} of 14.12µM (Table 2). In addition to their inhibitory activity against cancer cells, all the compounds were also tested for possible toxicity against non-cancer origin human embryonic kidney cell line, HEK-293. None of the compounds showed significant inhibition suggesting that all compounds were devoid of non-specific cytotoxicity and relatively safe. Based on the comparative cancer cell inhibition potential, most active compound **6o** was selected for further analysis.

Table 2 Cancer cell inhibition activity of compounds

Compound No.	Activity in terms of IC_{50} (Mean± SEM, in µM)			
	MCF-7	MDA-MB-231	ISHIKAWA	HEK-293
6h	>50	>50	>50	>50
6l	15.82±4.60	17.33±5.44	>50	49.73±2.40
6o	15.40±2.13	14.12±3.69	34.48±7.26	42.65±1.75

3.4. Compound 6o induces cell cycle arrest at G_0/G_1 in MDA-MB-231 cells

PI is cell impermeable water soluble DNA intercalating dye. The amount of bound dye fluorescence correlates with the content of DNA within a given cell. The relative content of DNA in a cell can be used to classify a population into groups of cells according to their current phase of the cell cycle using flow cytometry into G_0/G_1, S, and G_2/M. Cells in G_0/G_1 phases of the cell cycle are diploid (2n) containing a normal quantity of DNA, cells in G_2/M phases are tetraploid (4n) containing twice the amount of normal DNA content while cells in S-phase contains DNA greater than diploid cells and less than tetraploid cells. Cells having DNA content less than diploid is often termed as sub-diploid and are usually considered arising from apoptotic DNA. Here, when MDA-MB-231 cells were treated with **6o**, there was significant accumulation of cells at G_0/G_1 phase in a dose-dependent manner (Fig. 4A). Compound **6o** induced significant increase at the concentrations of 10µM ($P<0.01$), 14.12µM ($P<0.001$) and 18µM ($P<0.001$) as compared to untreated control suggesting **6o** induces G_0/G_1 arrest in MDA-MB-231 cells. As expected, there was also concomitant significant decrease in S-phase and G_2/M phase population in compound **6o** treated MDA-MB-231 cells as compared to untreated control group.

3.5. Compound 6o induces apoptosis in MDA-MB-231 cells

In living cells, phosphatidylserine is localized inside of the lipid bilayer. At the onset of apoptosis, phosphatidylserine is mobilized to the external portion of the membrane and becomes accessible for Annexin V-FITC binding. On the other hand, cellular DNA in a healthy live cell or early apoptotic cell is not accessible to binding of cell impermeable PI dye and therefore, any binding of PI suggests a compromise of the cell membrane as seen in late apoptosis or necrosis. Compound **6o** induced significant increase in both early apoptotic (Annexin V-FITC positive and PI negative) ($P<0.001$) and late apoptotic (Annexin V-FITC positive and PI positive) ($P<0.001$) cells (Fig. 4B). The mean total apoptotic is significantly enhanced with compound **6o** treatment in a concentration-dependent manner from 5.8% in untreated

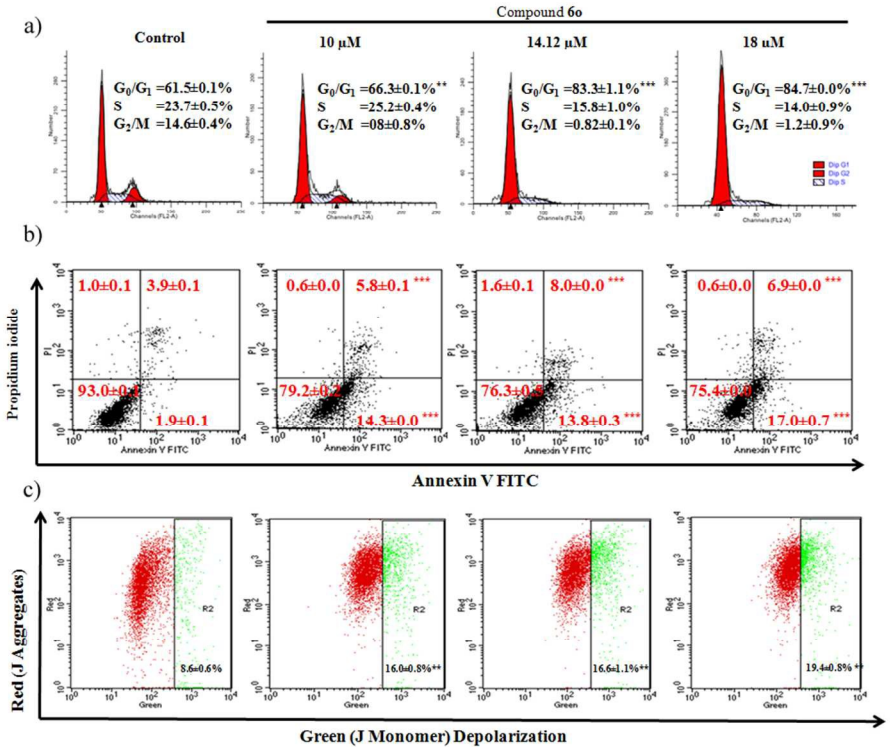

Fig. 4 a) Compound **6o** induced cell cycle arrest in MDA-MB-231 cells**.** Data are expressed as % of total cell count. **b**) Induced apoptosis in MDA-MB-231 cells**.** Data are expressed as % of total cell count. **c**) Induced mitochondrial membrane depolarization in MDA-MB-231 cells.

View Article Online
DOI: 10.1039/C6RA15674F

control to 20.1% at 10μM (P<0.001 *vs* untreated), 21.8% at 14.12μM (P<0.001 *vs* untreated) and 23.9% at 18μM (P<0.001 versus untreated).

3.6. Compound 6o induces mitochondrial membrane depolarization in MDA-MB-231 cells

Mitochondria play a major role in apoptosis, and its membrane potential destabilization is hallmark indicator of its involvement in intrinsic apoptosis pathway. JC-1 dye form J-aggregates in normal cellular Δψ and emits red fluorescence, while cells with low Δψ promote J-monomer formation that emits green fluorescence. Compound **6o** significantly enhanced the green fluorescence in dose dependent manner which is indicative of the depolarization of mitochondrial membrane potential in cells as compared to non-treated control group cells (P<0.01) (Fig. 4C). Out of three tested compounds, **6l** and **6o** were found to possess anticancer activity among which compound **6o** showed promising anticancer effect in breast cancer cells.

In view of the fact that, increased osteoclast number and decreased osteoblast count is the hallmark of bone metastasized osteoporosis, we next assessed the effect of these compounds on the osteoclast gene expression.

3.7. Effect of compounds 6h, 6l and 6o on osteoclast gene expression

Subsequently, we assayed the effect of these compounds on anti-osteoclastic activity by analysing real-time PCR of *TRAP* gene. Tartrate-resistant acid phosphatase (TRAP), once considered being a marker of osteoclasts, and it is able to degrade skeletal phosphoproteins and mineralization.

The relative mRNA levels of TRAP were found to be decreased at 1 μM (P < 0.01) (Fig. 5) concentrations in the presence of compound **6o** when compared to control cells TRAP. Above findings, altogether, demonstrates that compound **6o** showed anti-cancer activity as well as osteogenic properties. Hence, we selected compound **6o** to verify our hypothesis by means of *in-vitro* model of bone metastasis.

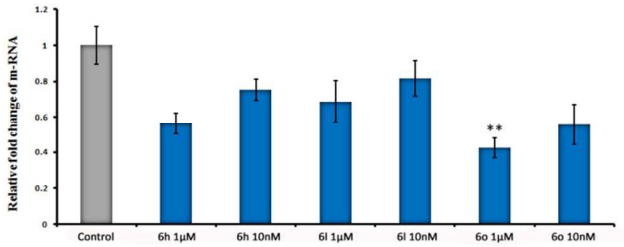

Fig. 5 Effect of Compounds **6h**, **6l** and **6o** on osteoclastogenesis from BMCs by relative mRNA expression of *TRAP* determined by *q*PCR and normalized with GAPDH.

3.8. Effect of compound 6o on bone marrow cells by bone metastatic model

Co-cultures of bone marrow cells and metastasis breast cancer cells provide a suitable experimental approach to study the effect of compounds combined with both types of cells *viz*. osteoblasts and cancer cells. Typically cancer cells secrete osteolytic factors that lead to net bone loss and on the other hand increases osteoclasts number that increases bone resorption. To analyze the effect of breast cancer cell on bone mineralization, we co-cultured the bone marrow cells in osteoblastic lineages in presence or absence of compound **6o** for eighteen days.

We found that bone marrow mineralization process was suppressed significantly (P < 0.001) in the presence of co-cultured cancer cells whereas bone mineralization suppression was inhibited by the presence of compound **6o** at 1 μM (P < 0.01) concentration. On the other hand, cancer cells co-cultured with bone marrow cells stimulated significantly (P < 0.001) bone marrow osteoclastogenesis compared to their respective control.These results indicated that breast cancer cells increase osteoclastogenesis that leads to increasing bone resorption. Treatment of compound **6o** at 1 μm significantly (P < 0.01) suppressed osteoclastogenesis that was enhanced by MDA-MB-231 breast cancer cells (Fig. 6).

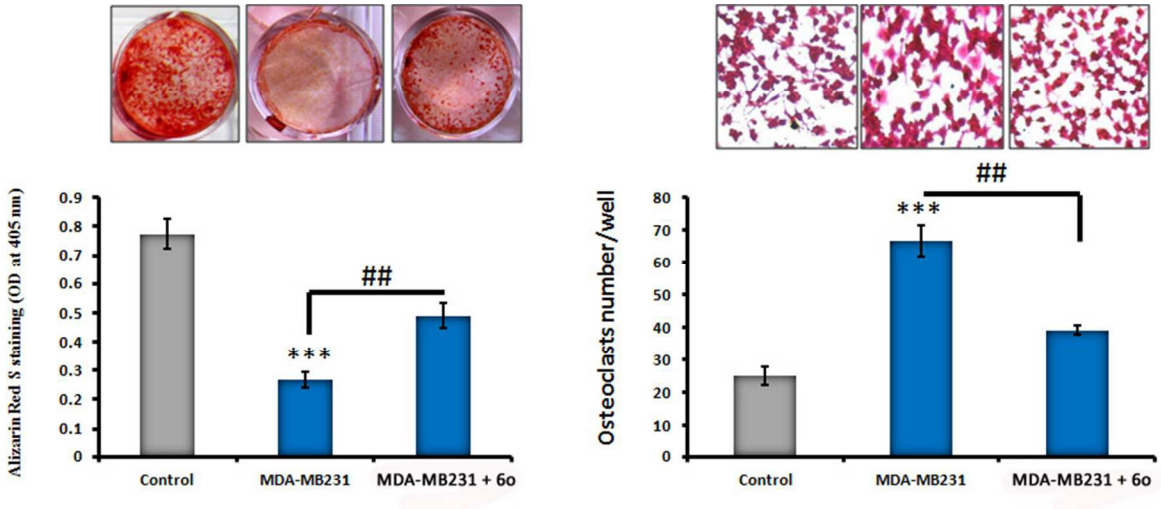

Fig. 6 Compound **6o** inhibit suppression of osteoblastic mineralization and suppresses osteoclastogenesis in the bone marrow cells of normal mice *in vitro* when cultured with MD-MBA 231 cells.

View Article Online
DOI: 10.1039/C6RA15674F

4. Conclusions

Breast cancer cells metastasize to the skeletal tissue thus leading to bone loss by osteolysis. The current therapies for bone loss are directed towards inhibition of osteoclasts, and recuperating osteoblasts. Eighteen compounds of coumarin-imidazo[1,2-*a*]pyridine hybrids with various modification were synthesized and evaluated for their various biological activity like osteogenesis, osteoclastogenesis and bone metastasis study. Out of all synthesized hybrids, compound **6h**, **6l**, and **6o** showed significantly increased ALP activity in mice calvarial osteoblasts cells. Further analysis revealed that these compounds increased mineralization and the expression of osteogenic genes. Out of the three compounds tested for anti-breast cancer activity, compound **6o** was found to be most active against MDA-MB-231 cells with IC_{50} of 14.12 ± 3.69 μM. Lead compound **6o** induced significant cell cycle arrest in MDA-MB-231 cells at G_0/G_1 phase with a concomitant reduction in S-phase and G_2/M phase. The active compound **6o** also induced significant apoptosis in MDA-MB-231 cells which are associated with mitochondrial depolarization. In addition, we showed co-culture of MDA-MB-231 with bone marrow cells disrupts bone homeostasis by deregulating the differentiation of osteoblast and osteoclast cells, and this disorder was recuperated by compound **6o**. This study indicates compound **6o** as promising lead for the development of new class of osteo-protective agents.

5. Experimental section

5.1. Analysis and instruments

All reagents were commercial and were used without further purification. Chromatography was carried on silica gel (60-120 and 100-200 mesh). All reactions were monitored by thin-layer chromatography (TLC), silica gel plates with fluorescence F254 were used. Melting points were taken in open capillaries on Complab melting point apparatus and are presented uncorrected. Infrared spectra were recorded on a Perkin-Elmer FT-IR RXI spectrophotometer. ^{1}H NMR and ^{13}C NMR spectra were recorded using Bruker Supercon Magnet DRX-300 spectrometer (operating at 400 MHz, 300 MHz for ^{1}H and 75 MHz for ^{13}C) using CDCl3 as solvent and tetramethylsilane (TMS) as internal standard. Chemical shifts are reported in parts per million and multiplicity(s = singlet, brs = broad singlet, d = doublet, brd = broad doublet, dd = double doublet, t = triplet, q = quartet, m = multiplet). Electro spray ionization mass spectra (ESIMS) were recorded on Thermo Lcq Advantage Max-IT. High resolution mass spectra (HRMS) were recorded on 6520 Agilent Q Tof LC-MS/MS (Accurate mass).

5.1.1. Representative procedure for the synthesis of compounds

2-Methyl/2-*Iso*-propyl/2-*Sec*-butyl/2-*Tert*-butyl phenol (1 equiv) and hexamethylenetetramine (1.2 equiv) were dissolved in TFA (25 mL) and the solution was heated at 120 °C for 6-8 h. After cooling to room temperature 10% aq. H_2SO_4 (40 mL) was added and again the temperature was maintained at 90 °C for 4 h. The solution was neutralized with $NaHCO_3$ and extracted with EtOAc. The combined organic layers were dried on Na_2SO_4, filtered, and concentrated to dryness under reduced pressure. The crude products were purified over silica gel column chromatography (60-120 mesh) to afford required compounds. (See supplementary info.)

5.1.2. Representative procedure for the synthesis of compounds 4a-4f:

A solution of 4-hydroxy-5-methylisophthalaldehyde (1.0 g, 6.1 mmol) and diethyl malonate (1.02 g, 6.38 mmol) in ethanol (20 mL) was treated with piperidine (0.2 mL) and refluxed for 1 hour. After the completion of the reaction, most of the solvent was evaporated under vacuum, and the piperidine was neutralized with glacial acetic acid. Water was added to the residue and extracted with three folds of 20 mL of DCM. The combined organic layers were dried over anhydrous Na_2SO_4, filtered, and concentrated to dryness under reduced pressure. The crude product thus obtained was purified by column chromatography to furnish compound **4a** with 78% yield. (See supplementary info.)

*Methyl 6-formyl-8-isopropyl-2-oxo-2H-chromene-3-carboxylate (**4b**):* White solid; Yield 81%; mp 104-106 °C; IR (KBr): 3042, 1730, 1615, 1024 cm^{-1}. ^{1}H NMR (400 MHz, $CDCl_3$) δ 10.04 (s, 1H), 8.61 (s, 1H), 8.09 (d, J = 1.7 Hz, 1H), 7.97 (d, J = 1.8 Hz, 1H), 3.97 (s, 3H), 3.68 – 3.63 (m, 1H), 1.35 (d, J = 6.9 Hz, 6H); ^{13}C NMR (100 MHz, $CDCl_3$) δ 190.1, 163.3, 156.3, 155.7, 148.9, 138.4, 133.0, 131.1, 129.9, 118.8, 118.0, 53.1, 26.7, 22.5; ESI-MS (m/z): 275 $(M+H)^+$

*Ethyl 6-formyl-8-isopropyl-2-oxo-2H-chromene-3-carboxylate (**4c**):* White solid; Yield 85%; mp: 117-119 °C; IR (KBr): 3038, 1722, 1620, 1022 cm^{-1}; ^{1}H NMR (400 MHz, $CDCl_3$) δ 10.03 (s, 1H), 8.57 (s, 1H), 8.08 (s, 1H), 7.97 (d, J = 1.5 Hz, 1H), 4.43 (q, J = 7.1 Hz, 2H), 3.65 (dt, J = 13.8, 6.9 Hz, 1H), 1.42 (t, J = 7.1 Hz, 3H), 1.35 (d, J = 6.9 Hz, 6H); ^{13}C NMR (100 MHz, $CDCl_3$): δ 190.1, 162.7, 156.2, 155.8, 148.4, 138.3, 132.9, 131.0, 129.9, 119.2, 118.0, 62.3, 26.8, 22.4, 14.3; ESI-MS (m/z): 289 $(M+H)^+$

5.1.3. General procedure for the synthesis of coumarin-imidazo[1,2-*a*]pyridine derivatives 6a-6r:

Silver triflate (20 mol%) was added to a mixture of ethyl 6-formyl-8-methyl-2-*oxo*-2*H*-chromene-3-carboxylate (**4a**) (1.0 equiv) 2-Amino-4-picoline (**5b**) (1.0 equiv) and *tert*-Butyl isocyanide (1.5 equiv) in ethanol, and the reaction was stirred at 80 °C for 6-8 hrs. After completion of reaction as indicated by TLC, solvent was evaporated under reduced pressure. The residue was quince with water and extracted three times with 20mL ethyl acetate. The combined organic layers were dried over Na_2SO_4 and concentrated under vacuum. The obtained crude was purified by column chromatography to give the targeted product **6a** in good yield.

*Ethyl 6-(3-(tert-butylamino)-7-methylimidazo[1,2-a]pyridin-2-yl)-8-methyl-2-oxo-2H-chromene-3-carboxylate (**6a**):* Yellow solid; yield: 84%; mp 125-127 ºC; IR (KBr): 3400, 3019, 1650, 1215, 669 cm^{-1}; ^{1}H NMR (400 MHz, CDCl3) δ 8.54 (s, 1H), 8.24 – 8.23 (m, 1H), 8.11 (d, J = 1.8 Hz, 1H), 8.05 (d, J = 7.0 Hz, 1H), 7.29 (s, 1H), 6.64 (dd, J = 7.0, 1.6 Hz, 1H), 4.42 (q, J = 7.1 Hz, 2H), 2.52 (s, 3H), 2.40 (s, 3H), 1.42 (t, J = 7.1 Hz, 3H), 1.08 (s, 9H).; ^{13}C NMR (100 MHz, $CDCl_3$) δ 163.3, 157.0, 152.7, 149.1, 142.7, 137.0, 135.6, 135.3, 132.0, 126.1, 123.0, 122.5, 117.9, 117.5, 115.7, 114.4, 61.9, 56.4, 30.5, 21.2, 15.4, 14.2; HRMS (ESI) calcd for $C_{25}H_{27}N_3O_4$ $[M + H]^+$ 434.2074, found 434.2075.

*Ethyl 6-(3-(tert-butylamino)imidazo[1,2-a]pyridin-2-yl)-8-methyl-2-oxo-2H-chromene-3-carboxylate (**6b**):* Yellow solid; yield: 82%; mp 145-147 ºC; IR (KBr): 3400, 3019, 1626, 1216, 669 cm^{-1};^{1}H NMR (400 MHz, $CDCl_3$) δ 8.63 (s, 1H), 8.15 (d, J =

View Article Online
DOI: 10.1039/C6RA15674F

6.9 Hz, 1H), 8.01 (d, *J* = 1.4 Hz, 1H), 7.93 (s, 1H), 7.29 (d, *J* = 9.1 Hz, 1H), 7.18 – 7.12 (m, 1H), 6.81 (t, *J* = 6.7 Hz, 1H), 4.44 (q, *J* = 7.1 Hz, 2H), 2.40 (s, 3H), 1.45 (t, *J* = 7.1 Hz, 3H), 0.97 (s, 9H); ^{13}C NMR (100 MHz, $CDCl_3$) δ 163.3, 157.8, 152.5, 149.0, 141.9, 139.3, 134.5, 131.1, 126.7, 126.2, 125.8, 124.6, 124.0, 118.4, 117.6, 116.2, 112.2, 62.1, 56.3, 30.3, 15.4, 14.2; HRMS (ESI) calcd for $C_{24}H_{25}N_3O_4$ $[M + H]^+$ 420.1918, found 420.1914.

Ethyl 6-(3-(tert-butylamino)-6-chloroimidazo[1,2-a]pyridin-2-yl)-8-methyl-2-oxo-2H-chromene-3-carboxylate ***(6c)****:* Yellow solid; yield: 77%; mp 118-120 ºC; IR (KBr): 3393, 3019, 1620, 1215, 669 cm^{-1}; ^{1}H NMR (400 MHz, $CDCl_3$) *δ* 8.54 (s, 1H), 8.22 (dd, *J* = 2.0, 0.8 Hz, 1H), 8.19 (dd, *J* = 2.0, 0.8 Hz, 1H), 8.07 (d, *J* = 1.9 Hz, 1H), 7.48 (dd, *J* = 9.5, 0.7 Hz, 1H), 7.14 (dd, *J* = 9.5, 2.0 Hz, 1H), 4.43 (q, *J* = 7.1 Hz, 2H), 2.99 (bs, 1H), 2.53 (s, 3H), 1.42 (t, *J* = 7.1 Hz, 3H), 1.09 (s, 9H); ^{13}C NMR (100 MHz, $CDCl_3$) δ 163.4, 156.9, 153.0, 149.0, 140.6, 138.7, 135.3, 131.5, 126.4, 126.3, 126.1, 124.0, 121.3, 120.4, 118.2, 117.9, 117.7, 62.0, 56.7, 30.7, 15.5, 14.3; HRMS (ESI) calcd for $C_{24}H_{24}ClN_3O_4$ $[M + H]^+$ 454.1528, found 454.1521.

Ethyl 6-(6-bromo-3-(tert-butylamino)imidazo[1,2-a]pyridin-2-yl)-8-(sec-butyl)-2-oxo-2H-chromene-3-carboxylate ***(6d)****:* Yellow solid; yield: 74%; mp 141-143 ºC; IR (KBr): 3399, 3019, 1619, 1216, 669 cm^{-1}; ^{1}H NMR (400 MHz, $CDCl_3$) δ 8.56 (s, 1H), 8.32 – 8.31 (m, 1H), 8.19 (d, *J* = 1.9 Hz, 1H), 8.07 (d, *J* = 2.0 Hz, 1H), 7.45 (d, *J* = 9.4 Hz, 1H), 7.23 (dd, *J* = 9.4, 1.9 Hz, 1H), 4.42 (q, *J* = 7.1 Hz, 2H), 3.51 – 3.42 (m, 1H), 2.99 (bs, 1H), 1.78 – 1.71 (m, 2H), 1.41 (t, *J* = 7.1 Hz, 3H), 1.33 (d, *J* = 6.9 Hz, 3H), 1.07 (s, 9H), 0.88 (t, *J* = 7.4 Hz, 3H); ^{13}C NMR (100 MHz, $CDCl_3$) δ 163.4, 156.9, 152.3, 149.3, 140.7, 138.9, 135.6, 132.1, 131.7, 128.1, 126.5, 123.93, 123.6, 118.2, 118.0, 106.9, 62.0, 56.7, 33.5, 30.6, 30.0, 20.7, 14.3, 12.2; HRMS (ESI) calcd for $C_{27}H_{30}BrN_3O_4$ $[M + H]^+$ 540.1492, found 540.1486.

Ethyl 8-(sec-butyl)-6-(3-(tert-butylamino)-6-chloroimidazo[1,2-a]pyridin-2-yl)-2-oxo-2H-chromene-3-carboxylate ***(6e)****:* Yellow solid; yield: 75%; mp 132-134 ºC; IR (KBr): 3399, 3019, 1621, 1215, 669 cm^{-1}; ^{1}H NMR (400 MHz, $CDCl_3$) δ 8.56 (s, 1H), 8.22 (d, *J* = 1.4 Hz, 1H), 8.19 (d, *J* = 1.9 Hz, 1H), 8.07 (d, *J* = 2.0 Hz, 1H), 7.50 (d, *J* = 9.5 Hz, 1H), 7.14 (dd, *J* = 9.5, 2.0 Hz, 1H), 4.43 (q, *J* = 7.1 Hz, 2H), 3.50 – 3.44 (m, 1H), 2.99 (s, 1H), 1.79 – 1.70 (m, 2H), 1.41 (t, *J* = 7.1 Hz, 3H), 1.33 (d, *J* = 6.9 Hz, 3H), 1.07 (s, 9H), 0.88 (t, *J* = 7.4 Hz, 3H); ^{13}C NMR (100 MHz, $CDCl_3$) δ 163.3, 156.9, 152.3, 149.3, 140.6, 139.1, 135.5, 132.1, 131.8, 126.5, 126.0, 124.1, 121.3, 120.4, 118.1, 117.9, 61.9, 56.7, 33.5, 30.5, 29.9, 20.7, 14.3, 12.2; HRMS (ESI) calcd for $C_{27}H_{30}ClN_3O_4$ $[M + H]^+$ 496.1998, found 496.1988.

Ethyl 6-(6-bromo-3-(tert-butylamino)imidazo[1,2-a]pyridin-2-yl)-8-(tert-butyl)-2-oxo-2H-chromene-3-carboxylate ***(6f)****:* Yellow solid; yield: 74%; mp 149-151 ºC; IR (KBr): 3395, 3021, 1580, 1216, 670 cm^{-1}; ^{1}H NMR (400 MHz, $CDCl_3$) δ 8.56 (s, 1H), 8.34 (d, *J* = 2.0 Hz, 1H), 8.32 – 8.30 (m, 1H), 8.10 (d, *J* = 2.0 Hz, 1H), 7.45 (d, *J* = 9.4 Hz, 1H), 7.24 (dd, *J* = 9.4, 1.9 Hz, 1H), 4.43 (q, *J* = 7.1 Hz, 2H), 2.99 (s, 1H), 1.57 (s, 9H), 1.42 (t, *J* = 7.1 Hz, 3H), 1.09 (s, 9H); ^{13}C NMR (100 MHz, $CDCl_3$) δ 163.4, 156.4, 153.5, 149.7, 140.8, 139.0, 138.0, 132.0, 131.3, 128.1, 127.0, 123.8, 123.6, 118.6, 118.3, 117.8, 106.9, 62.0, 56.8, 35.4, 30.6, 29.9, 14.3; HRMS (ESI) calcd for $C_{27}H_{30}BrN_3O_4$ $[M + H]^+$ 540.1492, found 540.1486.

Ethyl 8-(sec-butyl)-6-(3-(tert-butylamino)-7-methylimidazo[1,2-a]pyridin-2-yl)-2-oxo-2H-chromene-3-carboxylate ***(6g)****:* Yellow solid; yield: 82%; mp 96-98 ºC; IR (KBr): 3399, 3019, 1585, 1216, 669 cm^{-1}; ^{1}H NMR (400 MHz, $CDCl_3$) δ 8.56 (s, 1H), 8.24 (d, *J* = 1.7 Hz, 1H), 8.10 (d, *J* = 1.7 Hz, 1H), 8.06 (d, *J* = 7.0 Hz, 1H), 7.30 (s, 1H), 6.65 (d, *J* = 7.0 Hz, 1H), 4.42 (q, *J* = 7.1 Hz, 2H), 3.51 – 3.44 (m, 1H), 2.95 (bs, 1H) 2.40 (s, 3H), 1.76 – 1.74 (m, 2H), 1.41 (t, *J* = 7.1 Hz, 3H), 1.33 (d, *J* = 6.9 Hz, 3H), 1.06 (s, 9H), 0.87 (t, *J* = 7.4 Hz, 3H); ^{13}C NMR (100 MHz, $CDCl_3$) δ 163.5, 157.1, 152.1, 149.6, 142.9, 137.5, 135.7, 135.3, 132.4, 132.2, 126.4, 123.1, 122.6, 118.0, 117.9, 115.9, 114.6, 62.0, 56.5, 33.5, 30.6, 30.0, 21.4, 20.8, 14.3, 12.2; HRMS (ESI) calcd for $C_{28}H_{33}N_3O_4$ $[M + H]^+$ 476.2544, found 476.2542.

Ethyl 8-(tert-butyl)-6-(3-(tert-butylamino)-6-chloroimidazo[1,2-a]pyridin-2-yl)-2-oxo-2H-chromene-3-carboxylate ***(6h)****:* Yellow solid; yield: 78%; mp 142-144 ºC; IR (KBr): 3385, 3022, 1675, 1211, 669 cm^{-1}; ^{1}H NMR (400 MHz, $CDCl_3$) δ 8.55 (s, 1H), 8.34 (d, *J* = 2.0 Hz, 1H), 8.21 (dd, *J* = 2.0, 0.8 Hz, 1H), 8.09 (d, *J* = 2.0 Hz, 1H), 7.49 (dd, *J* = 9.5, 0.7 Hz, 1H), 7.14 (dd, *J* = 9.5, 2.0 Hz, 1H), 4.43 (q, *J* = 7.1 Hz, 2H), 2.98 (bs, 1H), 1.56 (s, 9H), 1.42 (t, *J* = 7.1 Hz, 3H), 1.08 (s, 9H); ^{13}C NMR (100 MHz, $CDCl_3$) δ 163.5, 156.4, 153.5, 149.6, 140.7, 139.3, 138.0, 132.0, 131.4, 127.0, 126.1, 124.0, 121.3, 120.5, 118.6, 118.0, 117.8, 62.0, 56.8, 35.4, 30.7, 30.1, 14.3; HRMS (ESI) calcd for $C_{27}H_{30}ClN_3O_4$ $[M + H]^+$ 496.1998, found 496.1988.

Ethyl 8-(tert-butyl)-6-(3-(tert-butylamino)imidazo[1,2-a]pyridin-2-yl)-2-oxo-2H-chromene-3-carboxylate ***(6i)****:* Yellow solid; yield: 80%; mp 123-125 ºC; IR (KBr): 3400, 3019, 1620, 1215, 669 cm^{-1}; ^{1}H NMR (400 MHz, $CDCl_3$) δ 8.56 (s, 1H), 8.40 (d, *J* = 1.7 Hz, 1H), 8.18 (d, *J* = 6.8 Hz, 1H), 8.14 (d, *J* = 1.7 Hz, 1H), 7.55 (d, *J* = 9.0 Hz, 1H), 7.20 – 7.15 (m, 1H), 6.82 (t, *J* = 6.5 Hz, 1H), 4.42 (q, *J* = 7.1 Hz, 2H), 2.97 (bs, 1H), 1.56 (s, 9H), 1.42 (t, *J* = 7.1 Hz, 3H), 1.08 (s, 9H); ^{13}C NMR (100 MHz, $CDCl_3$) δ 163.5, 156.6, 153.3, 149.8, 142.4, 138.0, 137.8, 132.1, 131.8, 127.0, 124.7, 123.5, 123.3, 118.6, 117.6, 117.6, 111.9, 62.0, 56.7, 35.3, 30.6, 30.0, 14.3; HRMS (ESI) calcd for $C_{27}H_{31}N_3O_4$ $[M + H]^+$ 462.2387, found 462.2381.

Ethyl 8-(tert-butyl)-6-(3-(tert-butylamino)-7-methylimidazo[1,2-a]pyridin-2-yl)-2-oxo-2H-chromene-3-carboxylate ***(6j)****:* Yellow solid; yield: 86%; mp 133-135 ºC; IR (KBr): 3400, 3015, 1621, 1208, 669 cm^{-1}; ^{1}H NMR (400 MHz, $CDCl_3$) δ 8.56 (s, 1H), 8.38 (d, *J* = 2.0 Hz, 1H), 8.12 (d, *J* = 2.0 Hz, 1H), 8.05 (d, *J* = 7.0 Hz, 1H), 7.30 (s, 1H), 6.65 (dd, *J* = 7.0, 1.5 Hz, 1H), 4.42 (q, *J* = 7.1 Hz, 2H), 2.94 (bs, 1H), 2.40 (s, 3H), 1.56 (s, 9H), 1.42 (t, *J* = 7.1 Hz, 3H), 1.07 (s, 9H); ^{13}C NMR (100 MHz, $CDCl_3$) δ 163.5, 156.6, 153.2, 149.8, 142.9, 137.7, 137.6, 135.7, 132.1, 132.0, 126.9, 123.0, 122.6, 118.6, 117.5, 115.9, 114.6, 61.9, 56.6, 35.3, 30.6, 30.0, 21.4, 14.3; HRMS (ESI) calcd for $C_{28}H_{33}N_3O_4$ $[M + H]^+$ 476.2544, found 476.2542.

Ethyl 6-(3-(tert-butylamino)imidazo[1,2-a]pyridin-2-yl)-8-isopropyl-2-oxo-2H-chromene-3-carboxylate ***(6k)****:* Yellow solid; yield: 84%; mp 140-142 ºC; IR (KBr): 3398, 3020, 1617, 1211, 669 cm^{-1}; ^{1}H NMR (400 MHz, $CDCl_3$) δ 8.57 (s, 1H), 8.34 (d, *J* = 1.9 Hz, 1H), 8.19 (d, *J* = 6.9 Hz, 1H), 8.13 (d, *J* = 2.0 Hz, 1H), 7.56 (d, *J* = 9.0 Hz, 1H), 7.20 – 7.18 (m, 1H), 6.82 (td, *J* = 6.8, 1.0 Hz, 1H), 4.42 (q, *J* = 7.1 Hz, 2H), 3.72 – 3.65 (m, 1H), 1.42 (t, *J* = 7.1 Hz, 3H), 1.36 (d, *J* = 6.9 Hz, 6H), 1.08 (s, 9H); ^{13}C NMR (100 MHz, $CDCl_3$) δ 163.5, 157.1, 151.9, 149.5, 142.5, 136.4, 132.2, 131.6, 126.4, 124.7, 123.6, 123.3, 118.1, 118.0,

View Article Online
DOI: 10.1039/C6RA15674F

117.6, 111.9, 62.0, 56.7, 30.7, 26.8, 22.8, 14.4; HRMS (ESI) calcd for $C_{26}H_{29}N_3O_4$ [M + H]$^+$ 448.2231, found 448.2221.

ethyl 6-(3-(tert-butylamino)-7-methylimidazo[1,2-a]pyridin-2-yl)-8-isopropyl-2-oxo-2H-chromene-3-carboxylate ***(6l)****:* Yellow solid; yield: 81%; mp 159-161 ºC; IR (KBr): 3400, 3022, 1612, 1211, 669 cm^{-1}; ^{1}H NMR (400 MHz, $CDCl_3$) δ 8.57 (s, 1H), 8.30 (s, 1H), 8.11 (d, *J* = 2.0 Hz, 1H), 8.05 (d, *J* = 7.0 Hz, 1H), 7.28 (s, 1H), 6.64 (dd, *J* = 7.0, 1.5 Hz, 1H), 4.43 (q, *J* = 7.1 Hz, 2H), 3.71 – 3.62 (m, 1H), 2.41 (s, 3H), 1.42 (t, *J* = 7.1 Hz, 3H), 1.36 (d, *J* = 6.9 Hz, 6H), 1.06 (s, 9H); ^{13}C NMR (100 MHz, $CDCl_3$) δ 163.5, 157.1, 151.8, 149.5, 142.8, 137.4, 136.3, 135.8, 132.3, 131.4, 126.4, 123.2, 122.7, 118.0, 117.9, 115.8, 114.6, 62.0, 56.5, 30.6, 26.7, 22.8, 21.4, 14.3; HRMS (ESI) calcd for $C_{27}H_{31}N_3O_4$ [M + H]$^+$ 462.2387, found 462.2381.

ethyl 6-(3-(tert-butylamino)-6-chloroimidazo[1,2-a]pyridin-2-yl)-8-isopropyl-2-oxo-2H-chromene-3-carboxylate ***(6m)****:* Yellow solid; yield: 74%; mp 117-119 ºC; IR (KBr): 3388, 3020, 1623, 1218, 669 cm^{-1}; ^{1}H NMR (400 MHz, $CDCl_3$) δ 8.55 (s, 1H), 8.27 (d, *J* = 2.0 Hz, 1H), 8.22 (dd, *J* = 2.0, 0.8 Hz, 1H), 8.09 (d, *J* = 2.0 Hz, 1H), 7.50 (dd, *J* = 9.5, 0.8 Hz, 1H), 7.14 (dd, *J* = 9.5, 2.0 Hz, 1H), 4.43 (q, *J* = 7.1 Hz, 2H), 3.72 – 3.65 (m, 1H), 2.99 (bs, 1H), 1.42 (t, *J* = 7.1 Hz, 3H), 1.36 (d, *J* = 6.9 Hz, 6H), 1.09 (s, 9H); ^{13}C NMR (100 MHz, $CDCl_3$) δ 163.4, 156.9, 152.0, 149.3, 140.7, 139.1, 136.6, 131.8, 131.4, 126.4, 126.1, 124.1, 121.3, 120.5, 118.2, 118.0, 117.9, 62.0, 56.8, 30.7, 26.8, 22.8, 14.3; HRMS (ESI) calcd for $C_{26}H_{28}ClN_3O_4$ [M + H]$^+$ 482.1841, found 482.1838.

ethyl 6-(6-bromo-3-(tert-butylamino)imidazo[1,2-a]pyridin-2-yl)-8-isopropyl-2-oxo-2H-chromene-3-carboxylate ***(6n)****:* Yellow solid; yield: 72%; mp 105-107 ºC; IR (KBr): 3400, 3019, 1618, 1210, 669 cm^{-1}; ^{1}H NMR (400 MHz, $CDCl_3$) δ 8.55 (s, 1H), 8.31 (dd, *J* = 1.9, 0.8 Hz, 1H), 8.27 (d, *J* = 1.9 Hz, 1H), 8.09 (d, *J* = 2.0 Hz, 1H), 7.45 (dd, *J* = 9.4, 0.8 Hz, 1H), 7.23 (dd, *J* = 9.4, 1.9 Hz, 1H), 4.43 (q, *J* = 7.1 Hz, 2H), 3.72 – 3.65 (m, 1H), 2.99 (bs, 1H), 1.42 (t, *J* = 7.1 Hz, 3H), 1.36 (d, *J* = 6.9 Hz, 6H), 1.09 (s, 9H); ^{13}C NMR (100 MHz, $CDCl_3$) δ 163.4, 156.9, 152.0, 149.3, 140.8, 140.3, 138.9, 131.7, 131.4, 128.1, 126.5, 123.9, 123.6, 118.2, 118.2, 118.0, 106.9, 62.0, 56.8, 30.7, 26.8, 22.8, 14.4; HRMS (ESI) calcd for $C_{26}H_{28}BrN_3O_4$ [M + H]$^+$ 526.1336, found 526.1337.

methyl 6-(3-(tert-butylamino)-7-methylimidazo[1,2-a]pyridin-2-yl)-8-isopropyl-2-oxo-2H-chromene-3-carboxylate ***(6o)****:* Yellow solid; yield: 78%; mp 118-120 ºC; IR (KBr): 3402, 3012, 1642, 1218, 669 cm^{-1}; ^{1}H NMR (400 MHz, $CDCl_3$) δ 8.59 (s, 1H), 8.34 (s, 1H), 8.13 (s, 1H), 8.05 (d, *J* = 7.0 Hz, 1H), 7.31 (s, 1H), 6.65 (d, *J* = 6.9 Hz, 1H), 3.96 (s, 3H), 3.72 – 3.65 (m, 1H), 2.41 (s, 3H), 1.36 (d, *J* = 6.9 Hz, 6H), 1.07 (s, 9H); ^{13}C NMR (100 MHz, $CDCl_3$) δ 164.1, 157.1, 151.8, 150.0, 136.3, 135.7, 132.5, 131.7, 126.4, 122.6, 117.9, 117.6, 115.9, 114.6, 56.5, 52.9, 30.6, 26.7, 22.8, 21.4; HRMS (ESI) calcd for $C_{26}H_{29}N_3O_4$ [M + H]$^+$ 448.2231, found 448.2229.

methyl 6-(6-bromo-3-(tert-butylamino)imidazo[1,2-a]pyridin-2-yl)-8-(tert-butyl)-2-oxo-2H-chromene-3-carboxylate ***(6p)****:* Yellow solid; yield: 84%; mp 147-149 ºC; IR (KBr): 3400, 3012, 1618, 1220, 669 cm^{-1}; ^{1}H NMR (400 MHz, $CDCl_3$) δ 8.60 (s, 1H), 8.35 (s, 1H), 8.13 (s, 1H), 8.00 (s, 1H), 7.42 (d, *J* = 9.2 Hz, 1H), 7.24 (s, 1H), 3.98 (s, 3H), 3.39 (bs, 1H), 1.56 (s, 9H), 0.99 (s, 9H); ^{13}C NMR (100 MHz, $CDCl_3$) δ 163.6, 156.1, 153.5, 149.7, 140.2, 138.2, 131.2, 130.2, 129.6, 127.4, 125.3, 124.2, 118.5, 117.6, 117.2, 107.8, 58.1, 56.5, 52.9, 35.4, 30.1; HRMS (ESI) calcd for $C_{26}H_{28}BrN_3O_4$ [M + H]$^+$ 526.1336, found 526.1335.

methyl 8-(tert-butyl)-6-(3-(tert-butylamino)-6-chloroimidazo[1,2-a]pyridin-2-yl)-2-oxo-2H-chromene-3-carboxylate ***(6q)****:* Yellow solid; yield: 82%; mp 133-135 ºC; IR (KBr): 3408, 3012, 1618, 1210, 669 cm^{-1}; ^{1}H NMR (400 MHz, $CDCl_3$) δ 8.58 (s, 1H), 8.29 (s, 1H), 8.21 (s, 1H), 8.07 (s, 1H), 7.45 (d, *J* = 8.9 Hz, 1H), 7.14 – 7.10 (m, 1H), 3.97 (s, 3H), 3.11 (bs, 1H), 1.56 (s, 9H), 1.06 (s, 9H); ^{13}C NMR (100 MHz, $CDCl_3$) δ 163.9, 156.3, 153.4, 150.0, 140.5, 139.1, 138.0, 131.8, 131.2, 127.1, 126.2, 124.4, 121.5, 120.6, 118.5, 117.7, 117.4, 56.6, 52.9, 35.3, 30.6, 30.0; HRMS (ESI) calcd for $C_{26}H_{28}ClN_3O_4$ [M + H]$^+$ 482.1841, found 482.1840.

methyl 6-(6-bromo-3-(tert-butylamino)imidazo[1,2-a]pyridin-2-yl)-8-(sec-butyl)-2-oxo-2H-chromene-3-carboxylate ***(6r)****:* Yellow solid; yield: 78%; mp 139-141 ºC; IR (KBr): 3399, 3011, 1620, 1215, 669 cm^{-1}; ^{1}H NMR (400 MHz, $CDCl_3$) δ 8.61 (s, 1H), 8.33 (s, 1H), 8.04 (s, 1H), 8.00 (s, 1H), 7.40 (d, *J* = 8.5 Hz, 1H), 7.25 (d, *J* = 10.7 Hz, 1H), 3.98 (s, 3H), 3.49 – 3.44 (m, 1H), 1.75 – 1.70 (m, 2H), 1.34 (d, *J* = 6.5 Hz, 3H), 1.00 (s, 9H), 0.87 (d, *J* = 7.0 Hz, 3H); ^{13}C NMR (100 MHz, $CDCl_3$) δ 163.6, 156.7, 152.3, 149.5, 140.2, 138.4, 135.7, 131.4, 130.9, 129.1, 126.8, 125.3, 124.2, 118.0, 117.8, 117.2, 107.6, 58.0, 56.4, 52.9, 33.2, 30.1, 20.7, 12.1; HRMS (ESI) calcd for $C_{26}H_{28}BrN_3O_4$ [M + H]$^+$ 526.1336, found 526.1335.

5.2. Biological protocols

5.2.1. Ethical statement

All animal care and experimental procedures were approved by the Institutional Animal Ethics Committee (IAEC). All animal studies were conducted under approved protocol by the IAEC (IAEC 2015/32) of CSIR-Central Drug Research Institute, India.

5.2.2. ALP and mineralization activity of calvarial osteoblasts cells

Mice calvarial osteoblasts were isolated from 1-2 day old BALB/c mice (both sexes). Osteoblast cells were isolated by protocols published elsewhere. Briefly, surgical isolation of skull and the removal of adherent tissues followed by five sequential digestions at 37 °C in a solution containing 0.1% dispase and 0.1% collagenase. Cells released from the sequential digestions second to fifth digestions were collected and plated in α-MEM containing 10% FBS and 1% penicillin/streptomycin and plated in osteoblast differentiation medium and cultured in the presence or absence of compounds **6a-6r** for 48 h. After treatment, cells were freeze-thawed by first keeping them at -70 °C then bringing them to 37 °C by dry bath to determine the ALP activity.[26] The activity measured at OD 405nm with a microplate reader (Molecular Device, USA).

For mineralization activity mice calvarial osteoblast cells (2 × 104 cells/well in a 12-well plate) were cultured in the differentiation medium, consisting of complete growth medium with ascorbic acid (50 μg/mL) and β-glycerophosphate (10 mM). The culture media was changed after 48 hours up to eighteen days. Treatment with ALP active compounds **6h**, **6l**, and **6o** was given. At the end of the experiment time, cells were washed with PBS and fixed with 4% paraformaldehyde in PBS for 30 min. The fixed cells were stained with 40 mM (pH 4.5) Alizarin Red-S for 30 min. For quantification of Alizarin Red-S staining, 800 μL

View Article Online
DOI: 10.1039/C6RA15674F

of 10% (v/v) acetic acid was added to each well and scraped from the plate and transferred with 10% (v/v) acetic acid. After this the slurry was overlaid with 50 μL mineral oil (Sigma–Aldrich), heated to 85 °C for 5 min, and transferred to ice. Next, the slurry was centrifuged at 2000 rpm for 20 min, and 500 μL of the supernatant was removed to a new tube. Next, 200 μL of 10% (v/v) ammonium hydroxide was added to neutralize the acid and OD was taken at 405 nm in Elisa reader (Molecular Device, USA).[27]

5.2.3. Quantitative real-time polymerase chain reaction

Total RNA was extracted from osteoblast cells treated with different concentration of active compounds **6h**, **6l**, and **6o** and control, using TRIzol (Invitrogen). cDNA was synthesized from 500 ng total RNA with the Revert Aid H Minus first strand cDNA synthesis kit (Thermo Scientific, USA). SYBR Green (PURE GENE, Genetix Asia Limited) was used for quantitative determination of the mRNAs for *RUNX2*, *BMP2*, *OCN*, Collagen Type-1 and a housekeeping gene glyceraldehyde-3-phosphate dehydrogenase (*GAPDH*). Primer is designed using the Universal probe library (Roche Diagnostics) (Table 3). For real-time quantitative polymerase chain reaction (qPCR) of different genes, the cDNA was amplified with Light Cycler 480 (Roche Diagnostics Pvt. Ltd.). SYBR green dye was used in PCR buffer to incorporated in double-stranded DNA in the Light Cycler 480. GAPDH was used to normalize differences in qPCR.[22]

Table 3 List of primer sequence of genes used for real time PCR[a]

Gene	Primer sequence	Accession number
COL1	F-CATGTTCAGCTTTGTGGACCT R-GCAGCTGACTTCAGGGATGT	NM_007742.3
GAPDH	F-AGCTTGTCATCAACGGGAAG R-TTTGATGTTAGTGGGGTCTCG	DQ403054.1
BMP2	F-AGATCTGTACCGCAGGCACT R-GTTCCTCCACGGCTTCTTC	NM_007553.2
RUNX2	F-CCCGGGAACCAAGAAATC R-CAGATAGGAGGGGTAAGACTGG	AF053956.1
OCN	F-AGACTCCGGCGCTACCTT R-CTCGTCACAAGCAGGGTTAAG	NM_007541.2

[a]**Abbreviations:** *COL1 (collagen type I), GAPDH (Glyceraldehydes 3-phosphate dehydrogenase), BMP2 (bone morphogenetic protein 2), RUNX2 (Runt-related transcription factor 2),* OCN (osteocalcin, bone gamma carboxyglutamate protein bglap, ocn)

5.2.4. Osteoclastogenesis from bone marrow cells

BALB/c mice of four weeks old (ten mice, both sexes) were sacrificed, and long bones (femur and tibia) were isolated. Bone marrow was flushed out, centrifuged and pellet was re-suspended in DMEM containing 10% FCS, and then transferred to culture flask in growth culture medium containing MCSF (30 ng/µL) and RANKL (50 ng/µL) for one day at 5% carbon dioxide supply in 37 °C incubator. Next day, the free floating cells were collected and re-suspended in the culture medium. The cells were cultured in 48 well plate for eight days. Compound **6o** was added at various concentrations (control, 10 nM, and 1µM) on the first day of culture till eighth days of cell culture. For TRAP (tartrate resistant acid phosphatase) staining, cultured osteoclast cells were fixed in 4.0% paraformaldehyde and stained using substrate Naphthol AS-BI phosphate. TRAP enzyme containing osteoclast cells were stained pink. For qPCR expression of m-RNA cells were collected in TRIzol reagent (Invitrogen, USA) and RNA was isolated as per manufacturer's instructions. cDNA was synthesized by 250 ng total RNA by cDNA synthesis kit (Thermo Scientific, USA).[28]

5.2.5. Cell lines and maintenance

Cell lines MCF-7 (Estrogen receptor positive breast cancer), MDA-MB-231 (Estrogen receptor negative breast cancer), HEK-293 (human embryonic kidney cell) cells originally purchased from ATCC, USA and Ishikawa (Endometrial adenocarcinoma) is obtained from CSIR-CDRI cells repository and maintained in lab in Dulbecco's modified Eagle's medium (DMEM) with 1X antibiotic-antimycotic solution (A5955, Sigma) and 10% fetal bovine serum (Invitrogen) in humidified atmosphere of 5% CO_2, 95% air at 37 °C.[29]

5.2.6. Cytotoxicity assay by MTT (3-(4,5-Dimethylthiazol-2-yl)-2,5-diphenyltetrazolium bromide)

Cancer cell inhibition assay was carried out using MTT [3-(4,5-dimethylthiazol-2yl)-2,5-biphenyl tetrazolium bromide] which gets converted into a colored insoluble formazan precipitate by mitochondrial dehydrogenases present only in viable cells.[30] Cells were seeded (1×10^3 cells/well in 100μL of DMEM medium) in 96-well microculture plate and allowed to grow overnight attaining 50-60% confluence. Compounds were added in different concentrations in triplicates and incubated for 24 hours. At the end of incubation, 10μL of MTT solution (5 mg/mL in PBS) was added to each well and further incubated for 3 hours. At the end of incubation, the medium was completely removed, and formazan crystals were dissolved in 100μL DMSO with gentle shaking and absorbance at 540nm was measured using a microplate reader (Biorad, USA).

5.2.7. Cell cycle analysis

To determine the cell cycle distribution, 5 x 10^4 MDA-MB-231 cells/well were plated in 6 well plates and treated with various concentrations of compound **6o** for 24 h. After treatment, the cells were collected by gentle trypsinization, fixed in 70% chilled ethanol and kept at -20 °C overnight for fixation. Next day, cells were washed in PBS, resuspended in 1 mL of PBS containing 30 μg RNase and 40 μg PI and incubated at room temperature for 30 min.[31] Data were recorded using flow cytometer (FACSCaliber, Becton-Dickinson, USA) and analyzed using CellQuest software (Becton-Dickinson, USA).

5.2.8. Annexin V-FITC and PI assay

The apoptosis-inducing effect of compound **6o** was evaluated by Annexin V-FITC and PI binding assay using flowcytometry.[32] MDA-MB-231 cells (1×10^6) were seeded in 6 well plates and allowed to grow overnight. The medium was then, replaced with fresh complete medium containing 10 μM, 14.12 μM and 18 μM concentration of compound **6o**. Cells were further incubated for 24 h at 37 °C. At the end of incubation, cells from the supernatant as well as adherent monolayer cells were harvested and washed with PBS. Cells (1×10^5) were stained with Annexin V-FITC and propidium iodide using the Annexin V-PI apoptosis detection kit (Sigma). Flow cytometry was performed using a FACScan equipped with a single 488 nm argon laser (Becton Dickinson, USA). Annexin V-FITC signals were recorded using excitation and emission settings of 488 nm and 535 nm respectively (FL-1 channel) and PI signals with 488 nm and 610 nm respectively (FL-2 channel). Debris and clumps were gated out using forward

View Article Online
DOI: 10.1039/C6RA15674F

and orthogonal light scatter and analyzed using CellQuest software (Becton-Dickinson, USA).

5.2.9. Mitochondrial membrane potential (MMP) analysis

MMP ($\Delta\psi$) was determined using lipophilic cationic dye, JC-1 (5,5',6,6'-tetrachloro-1,1',3,3'-tetraethylbenzimidazolcarbocyanine iodide).[33] MDA-MB-231 cells were cultured in 6-well plates and treated with 10 μM, 14.12 μM and 18 μM concentrations of compound **6o** for 24h. Cells were harvested, washed twice with PBS and stained in 1 mL culture medium containing 5 mmol/L of JC-1 (Molecular Probes, USA) for 30 min at 37 °C. Cells were washed twice with PBS, resuspended in 300 μL of PBS for each sample, immediately followed by flow cytometry (FACS Calibur, Becton-Dickinson, San Jose, CA, USA) and analyzed using CellQuest software (Becton-Dickinson, USA).

5.2.10. Co-culture of bone marrow cells with breast cancer cells

To study the effects of cancer cells on osteogenesis, MDA-MB-231 cells were co-cultured with bone marrow cells of osteoblasts and osteoclasts lineages.[34] For osteoblastogenesis, bone marrow cells (2 X 10^6 /well) were cultured for three days, and then the cells were co-cultured with MDA-MB-231 cells/well (1 X 10^4) in DMEM containing ascorbic acid (50 μg/mL) and β-glycerophosphate (10 mM) in the presence or absence of compound **6o** for added sixteen days. Culture media was changed alternative day. After culture, cells were washed with PBS and stained with Alizarin red stain to determine mineralization as described above.

In osteoclastogenesis lineages experiments, bone marrow (5 X 10^6 cells/well) were cultured in medium for two days, and then co-cultured with MDA-MB-231 bone metastatic (1 X 10^4 cells/well) in medium containing DMEM containing 10 % FBS in the presence or absence of compound **6o** for added eight days. Culture media was changed after 48 hours. After the culture, TRAP staining was applied as described above.

5.2.11. Statistical analysis

***P<0.001, **P<0.01, *P<0.05 *vs* control (untreated cells). Data from at least three independent experiments were analyzed and expressed as mean ± SE. Statistical comparison of more than two groups was performed using one-way ANOVA with Newman-Keuls test. Statistically, the difference was considered significant if $P < 0.05$. Statistical analyses were carried out using Prism 3.0 (GraphPad Software Inc, USA).

Acknowledgements

The authors are grateful to the Director, CSIR-CDRI for her constant support and encouragement, Dr S. P. Singh for technical support, SAIF for NMR, IR, and Mass spectral data. The CSIR, New Delhi, is thanked for the award of Senior Research Fellowship to L.R.S, D.C, A.A, S.G, S.A and G.R.P. This is CDRI communication number 9297.

Notes and references

[a] *Medicinal and Process Chemistry Division, CSIR-Central Drug Research Institute, BS-10/1, Sector 10, Jankipuram Extension, Sitapur Road, Lucknow, 226031, India. Fax: +91 522 2771942; Tel: +91 9919317940; E-mail: sashidhar123@gmail.com; kv_sashidhara@cdri.res.in*

[b] *Endocrinology Division, CSIR-Central Drug Research Institute, BS-10/1, Sector 10, Jankipuram Extension, Sitapur Road, Lucknow, 226031, India.*

† Electronic Supplementary Information (ESI) available: [details of any supplementary information available should be included here]. See DOI: 10.1039/b000000x/

‡ Footnotes should appear here. These might include comments relevant to but not central to the matter under discussion, limited experimental and spectral data, and crystallographic data.

1 F. Loi, L. A. Cordova, J. Pajarinen, T. H. Lin, Z. Yao and S. B. Goodman, *Bone*, 2016, **86**, 119-130.

2 http://www.iofbonehealth.org/facts-statistics

3 (*a*) D. Goltzman, *Nat. Rev. Drug Discov.*, 2002, **1**, 784-796. (*b*) O. Johnell and J. A. Kanis, *Osteoporos. Int.*, 2006, **17**, 1726-1733. c) A. Lipton, R. Uzzo, R. J. Amato, G. K. Ellis, B. Hakimian, G. D. Roodman and M. R. Smith, *J. Natl. Compr. Canc. Netw.*, 2009, **7 Suppl 7**, S1-29; quiz S30.

4 (*a*) G. D. Roodman, *N. Engl. J. Med.*, 2004, **350**, 1655-1664.; (*b*) M. Futakuchi, K. Fukamachi and M. Suzui, *Adv. Drug Deliv. Rev.*, 2016, **99**, 206-211.

5 M. C. S. Khoon, *Adv. Drug Deliv. Rev.*, 2015, **94**, 141-150.

6 B. F. Boyce, T. Yoneda and T. A. Guise, *Endocr. Relat. Cancer*, 1999, **6**, 333-347.

7 (*a*) I. R. Hart, *Cancer Metastasis Rev.*, 1982, **1**, 5-16.; (*b*) I. J. Fidler, *Nat. Rev. Cancer*, 2003, **3**, 453-458.

8 K. A. Kennel and M. T. Drake, *Mayo Clin. Proc.*, 2009, **84**, 632-638.

9 T. Whitmarsh, G. M. Treece, A. H. Gee and K. E. S. Poole, *Plos One*, 2016, **11**, e0147722.

10 (*a*) W. Li, W. J. Chen and Y. Lin, *Medicine*, 2015, 94; (*b*) F. Cosman, *Bonekey Rep*, 2014, **3**, 518; (*c*) D. M. Black, S. L. Greenspan, K. E. Ensrud, L. Palermo, J. A. McGowan, T. F. Lang, P. Garnero, M. L. Bouxsein, J. P. Bilezikian, C. J. Rosen and T. H. S. I. Pa, *N. Engl. J. Med.*, 2003, **349**, 1207-1215; (*d*) J. S. Finkelstein, A. Hayes, J. L. Hunzelman, J. J. Wyland, H. Lee and R. M. Neer, *N. Engl. J. Med.*, 2003, **349**, 1216-1226.

11 M. Arisawa, S. S. Handa, D. D. McPherson, D. C. Lankin, G. A. Cordell, H. H. Fong and N. R. Farnsworth, *J. Nat. Prod.*, 1984, **47**, 300-307.

12 (*a*) J. S. Sun, Y. Y. Li, M. H. Liu and S. Y. Sheu, *J. Biomed. Mater. Res. A*, 2007, **81A**, 214-223; (*b*) S. Liu, D. Hsieh, Y. L. Yang, Z. Xu, C. Peto, D. M. Jablons and L. You, *BMC Pharmacol. Toxicol.*, 2013, **14**, 36.

13 (*a*) C. H. Tang, R. S. Yang, M. Y. Chien, C. C. Chen and W. M. Fu, *Eur. J. Pharmacol.*, 2008, **579**, 40-49.; (*b*) Y. M. Zheng, A. X. Lu, J. Z. Shen, A. H. Kwok and W. S. Ho, *Oncol. Rep.*, 2016, **35**, 1995-2002.

14 F. De Amicis, S. Aquila, C. Morelli, C. Guido, M. Santoro, I. Perrotta, L. Mauro, F. Giordano, A. Nigro, S. Ando and M. L. Panno, *Mol. Cancer*, 2015, **14**, 130.

15 U. Dutta and K. Pant, *Med. Oncol.*, 2008, **25**, 113-124.

16 (*a*) J. Cuzick, I. Sestak, S. Cawthorn, H. Hamed, K. Holli, A. Howell, J. F. Forbes and I.-I. Investigators, *Lancet Oncol.*, 2015, **16**, 67-75.; (*b*) I. Sestak, S. Singh, J. Cuzick, G. M. Blake, R. Patel, F. Gossiel, R. Coleman, M. Dowsett, J. F. Forbes, A. Howell and R. Eastell, *Lancet Oncol.*, 2014, **15**, 1460-1468.

17 (*a*) S. Demkowicz, J. Rachon, M. Dasko and W. Kozak, *RSC Adv*, 2016, **6**, 7101-7112.; (*b*) P. Clezardin, *Bonekey Rep.*, 2013, **2**, 267; (*c*) P. Clezardin, I. Benzaid and P. I. Croucher, *Bone*, 2011, **49**, 66-70; (*d*) P. Clezardin, *Bone*, 2011, **48**, 71-79.

18 (*a*) D. P. Nichols, K. N. Kuk and J. A. Nick, *Curr. Opin. Pulm. Med.*, 2015, **21**, 617-625; (*b*) T. Eley, T. Garimella, W. Y. Li and R. J. Bertz, *Clin. Pharmacokinet.*, 2015, **54**, 1205-1222; (*c*) K. C. Bulusu, R. Guha, D. J. Mason, R. P. I. Lewis, E. Muratov, Y. K. Motamedi, M. Cokol and A. Bender, *Drug Discov. Today*, 2016, **21**, 225-238; (*d*) L. Lionetto, M. Borro, M. Curto, M. Capi, A. Negro, F. Cipolla, G. Gentile and P. Martelletti, *Expert Opin. Drug Metab. Toxicol.*, 2016, **12**, 399-406.

View Article Online
DOI: 10.1039/C6RA15674F

19 (*a*) L. F. Tietze, H. P. Bell and S. Chandrasekhar, *Angew. Chem. Int. Ed. Engl.*, 2003, **42**, 3996-4028; (*b*) B. Meunier, *Acc. Chem. Res.*, 2008, **41**, 69-77; (*c*) P. G. Baraldi, A. N. Zaid, D. Preti, F. Fruttarolo, M. A. Tabrizi, A. Iaconinoto, M. G. Pavani, M. D. Carrion, C. L. Cara and R. Romagnoli, *Arkivoc*, 2006, 20-34; (d) R. Sunke, P. V. Babu, S. Yellanki, R. Medishetti, P. Kulkarni and M. Pal, *Org. Biomol. Chem.*, 2014, **12**, 6800-6805; (e) K. V. Sashidhara, S. R. Avula, V. Mishra, G. R. Palnati, L. R. Singh, N. Singh, Y. S. Chhonker, P. Swami, R. S. Bhatta and G. Palit, *Eur. J. Med. Chem.*, 2015, **89**, 638-653; (f) K. V. Sashidhara, G. R. Palnati, L. R. Singh, A. Upadhyay, S. R. Avula, A. Kumar and R. Kant, *Green Chem.*, 2015, **17**, 3766-3770.

20 P. Manvar, F. Shaikh, R. Kakadiya, K. Mehariya, R. Khunt, B. Pandey and A. Shah, *Tetrahedron*, 2016, **72**, 1293-1300.

21 S. Karamthulla, M. N. Khan and L. H. Choudhury, *RSC Adv.*, 2015, **5**, 19724-19733.

22 K. V. Sashidhara, R. K. Modukuri, D. Choudhary, K. Bhaskara Rao, M. Kumar, V. Khedgikar and R. Trivedi, *Eur. J. Med. Chem.*, 2013, **70**, 802-810.

23 K. V. Sashidhara, S. R. Avula, P. K. Doharey, L. R. Singh, V. M. Balaramnavar, J. Gupta, S. Misra-Bhattacharya, S. Rathaur, A. K. Saxena and J. K. Saxena, *Eur. J. Med. Chem.*, 2015, **103**, 418-428.

24 (*a*) S. K. Guchhait and C. Madaan, *Synlett*, 2009, 628-632; (*b*) A. Shahrisa and S. Esmati, *Synlett*, 2013, **24**, 595-602; (*c*) S. Vidyacharan, A. H. Shinde, B. Satpathi and D. S. Sharada, *Green Chem*, 2014, **16**, 1168-1175.

25 (*a*) K. Groebke, L. Weber and F. Mehlin, *Synlett*, 1998, 661-663; b) K. B. Puttaraju and K. Shivashankar, *RSC Adv.*, 2013, **3**, 20883-20890.

26 (*a*) C. G. Bellows, J. E. Aubin and J. N. Heersche, *Bone Miner.*, 1991, **14**, 27-40.; (*b*) J. A. Siddiqui, G. Swarnkar, K. Sharan, B. Chakravarti, A. K. Gautam, P. Rawat, M. Kumar, V. Gupta, L. Manickavasagam, A. K. Dwivedi, R. Maurya and N. Chattopadhyay, *Osteoporosis Int.*, 2011, **22**, 3013-3027.

27 C. A. Gregory, W. G. Gunn, A. Peister and D. J. Prockop, *Anal Biochem.*, 2004, **329**, 77-84.

28 U. S. Singh, R. Shankar, A. Kumar, R. Trivedi, N. Chattopadhyay, N. Shakya, S. Palne, S. Gupta and K. Hajela, *Bioorg. Med. Chem.*, 2008, **16**, 8482-8491.

29 K. V. Sashidhara, J. N. Rosaiah, M. Kumar, R. K. Gara, L. V. Nayak, K. Srivastava, H. K. Bid and R. Konwar, *Bioorg. Med. Chem. Lett.*, 2010, **20**, 7127-7131.

30 A. Sharma, B. Chakravarti, M. P. Gupt, J. A. Siddiqui, R. Konwar and R. P. Tripathi, *Bioorg. Med. Chem.*, 2010, **18**, 4711-4720.

31 M. I. Ansari, M. K. Hussain, A. Arun, B. Chakravarti, R. Konwar and K. Hajela, *Eur. J. Med. Chem.*, 2015, **99**, 113-124.

32 K. Chauhan, A. Arun, S. Singh, M. Manohar, K. Chuttani, R. Konwar, A. Dwivedi, R. Soni, A. K. Singh, A. K. Mishra and A. Datta, *Bioconjug. Chem.*, 2016, **27**, 961-972.

33 K. Upadhyaya, Hamidullah, K. Singh, A. Arun, M. Shukla, N. Srivastava, R. Ashraf, A. Sharma, R. Mahar, S. K. Shukla, J. Sarkar, R. Ramachandran, J. Lal, R. Konwar and R. P. Tripathi, *Org. Biomol. Chem.*, 2016, **14**, 1338-1358.

34 (*a*) S. Y. Park, H. J. Kim, K. R. Kim, S. K. Lee, C. K. Lee, K. K. Park and W. Y. Chung, *Toxicol. Appl. Pharmacol.*, 2014, **275**, 152-162; (*b*) M. Yamaguchi, S. Zhu, M. N. Weitzmann, J. P. Snyder and M. Shoji, *Mol. Cell Biochem.*, 2015, **401**, 1-10.

View Article Online
DOI: 10.1039/C6RA15674F

Table of Contents:

Design, synthesis and *in-vitro* evaluation of coumarin-imidazo[1,2-*a*]pyridine derivatives against cancer induced osteoporosis

Koneni V. Sashidhara,[a,*] L. Ravithej Singh,[a] Dharmendra Choudhary,[b] Ashutosh Arun,[b] Sampa Gupta,[a] Sulekha Adhikary,[b] Gopala Reddy Palnati,[a] Rituraj Konwar[b] and Ritu Trivedi[b]

[a]*Medicinal and Process Chemistry Division,* [b]*Endocrinology Division, CSIR-Central Drug Research Institute, BS-10/1, Sector 10, Jankipuram Extension, Sitapur Road, Lucknow, 226031, India.*

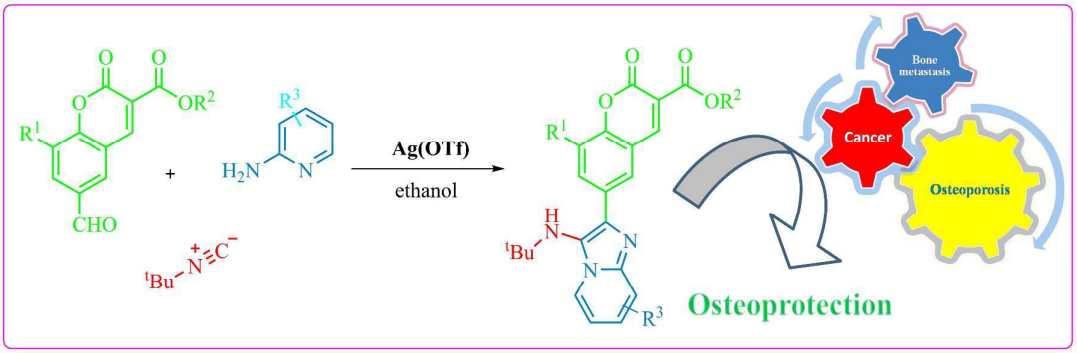

The potential of coumarin-imidazo[1,2-*a*]pyridine hybrids to prevent bone loss in patients with bone metastases is discussed.